Accepted Manuscript

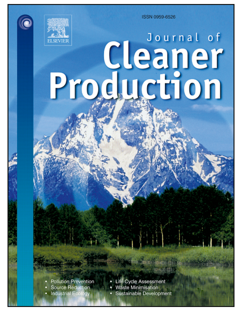

Sustainable aluminium recycling of end-of-life products: A joining techniques perspective

Vi Kie Soo, Jef Peeters, Dimos Paraskevas, Paul Compston, Matthew Doolan, Joost R. Duflou

PII: S0959-6526(17)33229-8

DOI: 10.1016/j.jclepro.2017.12.235

Reference: JCLP 11630

To appear in: *Journal of Cleaner Production*

Received Date: 16 June 2017

Revised Date: 9 November 2017

Accepted Date: 27 December 2017

Please cite this article as: Soo VK, Peeters J, Paraskevas D, Compston P, Doolan M, Duflou JR, Sustainable aluminium recycling of end-of-life products: A joining techniques perspective, *Journal of Cleaner Production* (2018), doi: 10.1016/j.jclepro.2017.12.235.

Word count: 7635 words

Sustainable Aluminium Recycling of End-of-Life Products: A Joining Techniques Perspective

Vi Kie Soo[a]*, Jef Peeters[b], Dimos Paraskevas[b], Paul Compston[a], Matthew Doolan[a], Joost R. Duflou[b]

[a] *Research School of Engineering, College of Engineering and Computer Science, The Australian National University, Canberra, ACT 2601, Australia*

[b] *KU Leuven, Department of Mechanical Engineering, Celestijnenlaan 300A, B-3001 Heverlee, Belgium*

* Corresponding author. Tel.: +6-126-125-5941; fax: +6-126-125-0506. *E-mail address:* vikie.soo@anu.edu.au

Abstract

The sustainable management of aluminium has become crucial due to the exponential growth in global demand. The transition to a sustainable society with lightweight electric vehicles has led to the increasing use of aluminium in the transportation sector. This has consequently led to the importance of aluminium recycling to prevent the valuable material stream going to landfill. In addition, the extraction of primary aluminium has high environmental impact due to the high energy consumption and waste generation in comparison to secondary aluminium processing. Despite being one of the most recycled metals, ongoing trends of multi-material designs and the associated joining choices have caused increasing difficulty of separating aluminium with high purity.

This paper evaluates the types of joining techniques causing impurities in the aluminium streams, and the relationship between particle size reduction and the presence of impurities due to joints particularly for end-of-life vehicles. An empirical experiment in a leading European recycling facility was conducted and demonstrated that mechanical fasteners, such as machine screws, socket screws, bolt screws and rivets, are the major types of joining technique causing impurities. Based on the observations from this case study, the characteristics of imperfectly liberated joints are examined. A Life Cycle Assessment (LCA) is also performed to evaluate the environmental impact of recycling different aluminium scrap qualities with varying impurity levels. The outcomes are then used to

provide ecodesign guidelines aimed at improving the quality and increase the quantity of recycled aluminium.

Keywords

Joining technologies; Al recycling; End-of-Life; recycling efficiency; ecodesign; Life Cycle Assessment

1 Introduction

Aluminium (Al) is used in a variety of products due to its high strength-to-weight ratio, good formability, and high corrosion resistance. The global demand for Al has seen significant growth, leading to the importance of sustainable metal management. The amount of Al used globally has been increasing since 1950, as can be seen in Figure 1, and this trend is projected to continue (Cullen and Allwood, 2013; Martchek, 2006). One of the major concerns is the continuous energy-intensive extraction of primary Al to supply for the growing demand worldwide. This activity has contributed significantly to the global carbon dioxide emissions (Norgate et al., 2007). Although Al is one of the highly recycled metals, offering significant energy saving during secondary production, the benefits of Al recycling are influenced by the purity level of scrap sources (Liu and Müller, 2012).

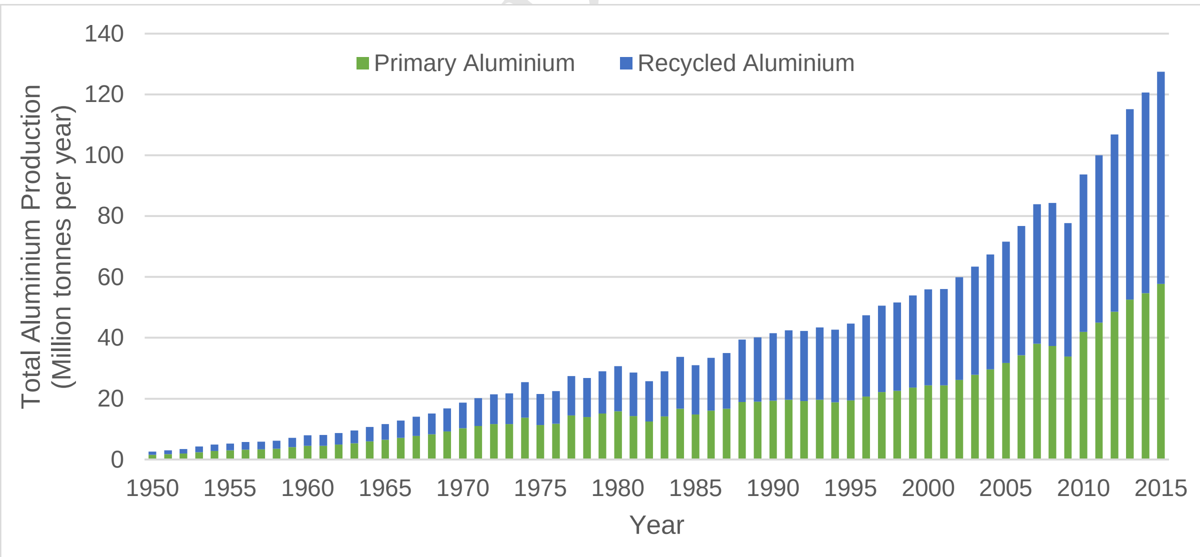

Figure 1: Amount of primary and recycled Al used globally (International Aluminium Institute, 2017).

The transportation industry is one of the major consumers of Al worldwide and is responsible for 35-40% of the overall Al consumption (Nappi, 2013). In recent years, the focus on producing lightweight vehicles has led to the increasing use of high purity Al in vehicle design to replace conventional steels (Goede et al., 2008). Multi-material design concepts have been progressively adopted by vehicle manufacturers due to the emphasis on reducing vehicle mass, thereby lowering the vehicle carbon footprint (Cui et al., 2011; Miller et al., 2000). Al or Al alloys are among the most suitable material category candidates for the manufacture of multi-material car bodies for automotive applications such as Body-in-White (BIW), chassis components, doors closure and outer panels (Carle and Blount, 1999; Hirsch, 2011; Volkswagen Group, 2009).

1.1 Joining Trends in Multi-Material Products – An Example using Vehicle Design

The increasing use of multi-material products focussing on mass reduction has led to changing joining trends (Groche et al., 2014; Mori et al., 2013; Soo et al., 2015). For example, the material composition in newer vehicle designs has undergone significant transformation particularly with the use of light metals, such as Al (Barnes and Pashby, 2000a; Carle and Blount, 1999; Miller et al., 2000), and lightweight materials, such as plastics and composites (U.S Department of Energy, 2013). As a result, the choice of joining techniques that are feasible to combine these multi-material combinations is limited (Meschut et al., 2014). Although there are several ongoing developments in more advanced joining technologies, their application in large-scale production is still restricted due to the proven design requirements in this risk averse sector (Barnes and Pashby, 2000a, 2000b), and the additional manufacturing costs of installing new equipment (Davies, 2012). Table 1 shows that the Al-intensive vehicle spaceframe structures (Audi A6 and A8) have increased the use of some joining techniques, while reducing others. The large amount of wrought Al used for these luxury vehicles is expected to be adopted also in electric vehicle and mass-optimised vehicle designs. Hatayama et al. (2012) have predicted the increasing demand of wrought Al to produce the power-supply box in electric vehicles. The growing Al composition in vehicle designs has led to the increasing use of mechanical joining techniques, such as screws and rivets, and adhesive bonding. In contrast, traditional welding techniques (e.g. spot welding and MIG welding) are showing a decreasing trend. The observed joining trends are also supported by the vehicle manufacturers' viewpoint on the development of joining processes used for future large scale vehicle production (Grote and Antonsson, 2009).

Table 1: Joining trends of different vehicle models' spaceframe structure (Adapted from European Aluminium Association, 2013; Mirdamadi and Korchnak, n.d.).

Joint type	**Audi A6**		**Trend**	**Audi A8**		**Trend**
	2001-2004	**2005-2008**		**1994-2002**	**2009-present**	
Share of point joints (%)						
Spot welding	91.5	81.0	↓	28.1	7.5	↓
Stud welding	3.3	6.5	↑	0	0	
Clinching	0.9	1.3		10.0	0	↓
Screw joints	0	0		0	23.6	↑
Rivets	0	5.8	↑	61.9	68.9	↑
Share of linear joints (%)						
Laser welding	8.3	3.3	↓	0	8	↑
MIG welding	6	4.3	↓	100	33.3	↓
Laser brazing	0	3.1	↑	0	0	
Adhesive bonding	85.7	89.3	↑	0	58.7	↑

Perfect material separation during the end-of-life (EoL) phase is not possible in the shredder-based recycling practices due to the complex product designs and the difficulty in separating different material types from their associated joining techniques (Van Schaik and Reuter, 2007). Castro et al. (2005) and Van Schaik and Reuter (2007) have shown that the increasing complexity in vehicle designs further hinders perfect liberation of dissimilar materials. As a result, lower grades and qualities of recyclates will be retrieved due to the presence of impurities that lead to cascade recycling (Paraskevas et al., 2015) and the loss of valuable material streams. This is particularly the case for recycling Al scrap that has more limitations during metallurgical recycling in comparison to other metals such as iron and copper (Nakajima et al., 2010). One of the main reasons is the relatively low melting point of Al, which makes it difficult to remove impurities or tramp elements—contaminants affecting the quality of metals that are not added on purpose—during the secondary Al smelting and refining processes. The most common strategies used to address this challenge are either dilution using primary Al or down-cycling to lower grade Al alloys that are associated to additional environmental burden (Castro et al., 2004; Paraskevas et al., 2015). The ability to retrieve high quality Al with low impurities increases the scrap value for recyclers; however, the extra recycling costs need to be justified by the volume of different scrap qualities.

1.2 Generic Design Guidelines for Joining Choices

Most of the design rules specific to joining choices facilitate Design for Disassembly (DfD) for part repair or material reuse that may not cater well for destructive recycling (Ferrão and Amaral, 2006; Güngör, 2006; Kriwet et al., 1995; Reuter, 2011). Screwing, for example, is preferred over adhesive bonding to ease the maintenance and repair of highly complex products, as well as part reuse. However, most EoL products are put through a shredding process in industrialised regions. Consequently, screws may not be separated well from the base materials, particularly when they are used to combine different material types (Castro et al., 2005; Van Schaik and Reuter, 2007), whereas weak adhesive bonding might be easily released in a shredding process. With the increasing complexity of multi-material structures in products, there is a need to consider the implications of both product design and the choice of joining elements on the quality of recycled materials (Reuter, 2011).

There are a few ecodesign guidelines that provide advice on joint selection for destructive recycling, such as the "Ten Golden Rules" (Luttropp and Lagerstedt, 2006) and VDI 2243 design guidelines (VDI 2243, 1993). In spite of that, the details on joint selection are very generic. According to the 'golden rule number 10', joining elements should be minimal, and the use of screws, adhesives, welding, snap fits and geometric locking should be appropriate for different life cycle scenarios. In contrast, VDI 2243 and recycling guidelines by Bras (2005) differentiate the guidelines between disassembly and destructive recycling to assist designers in choosing the most appropriate product design based on the fastening principles.

The choice of joining techniques during the design phase is gaining prominence for the sustainability of high purity metal recycling due to the current recycling practices (Castro et al., 2005; Van Schaik and Reuter, 2007; Worrell and Reuter, 2014). Studies on the limitations of Al recycling are mostly focussed on the efficiency of current sorting and separation processes (Froelich et al., 2007; Gaustad et al., 2012) and the challenges during the metallurgical recycling phase (Nakajima et al., 2010; Paraskevas et al., 2015; Reck and Graedel, 2012). There is a lack of understanding of the influence of joining choices during initial product design on the quality of recycled Al that is retrieved from highly complex products.

This work investigates the types of joining techniques causing impurities in the Al streams when advanced recycling technologies are applied. The study is based on an industrial trial carried out in a leading recycler located in Belgium. Impurities due to joints are identified to understand to what extent they are affecting the collected Al streams. The observations are then expanded to assess the correlation between the presence of impurities due to specific joint types, and the different particle liberation sizes. Based on the case study data, a Life Cycle Assessment (LCA) is performed to evaluate the environmental impact of recycling different Al scrap qualities. This study assists manufacturers and designers to promote closed-loop recycling by mitigating the source of impurities through effective joining technology selection during the initial design stage that caters for current recycling practices. In addition, recyclers and policy-makers can target effective recycling processes and standards to ensure perfectly liberated joints for high purity Al to minimise the loss of valuable material streams.

2 Materials and Methods

This study analyses the cause of impurities present in the different Al output fractions sampled from a Belgium recycling facility. Section 2.1-2.3 describe the Al recycling processes and sampling procedures. To assess to what extent the impurities are affecting the environmental impact of recycling different Al scrap qualities, the LCA method is used, as detailed in Section 2.4.

2.1 Recovery of Aluminium in Belgium

The types of scrap sources as considered in the studied Belgian recycling facility, one of the leading recyclers in Europe, are shown in Table 2. The high content of Al in different scrap sources has made it one of the most intensely recycled metals besides steel. Most of the Al scrap is contributed by the end-of-life vehicle (ELV) and household waste streams. The Al content in the ELV and household waste accounts for 4.9wt.% (Muchová and Eder, 2010; RDC Environment, 2015) and 4.7wt.% (Muchová and Eder, 2010) respectively. The Al content in demolition and building scrap is relatively low, less than 1wt.% (Muchová and Eder, 2010).

Table 2: The sources of the Al containing scrap as recycled in the Belgian recycling facility.

Scrap sources	Relative share of total scrap stream (%)
Depolluted vehicle hulks (ELV)	30
Demolition scrap	30
Household waste	20
Building scrap	20

The material process flow specific to Al is shown in Figure 2. The processes involved in Al recycling can be categorised into three main clusters: Al sorting, refinement of sorted aluminium, and particle size sorting. For Al sorting, density separation is the first step to retrieve Al from the mixture of scrap. Subsequently, other major processes, such as eddy current separator, optical separator, and head pulley magnet, are used to further separate Al from other material types.

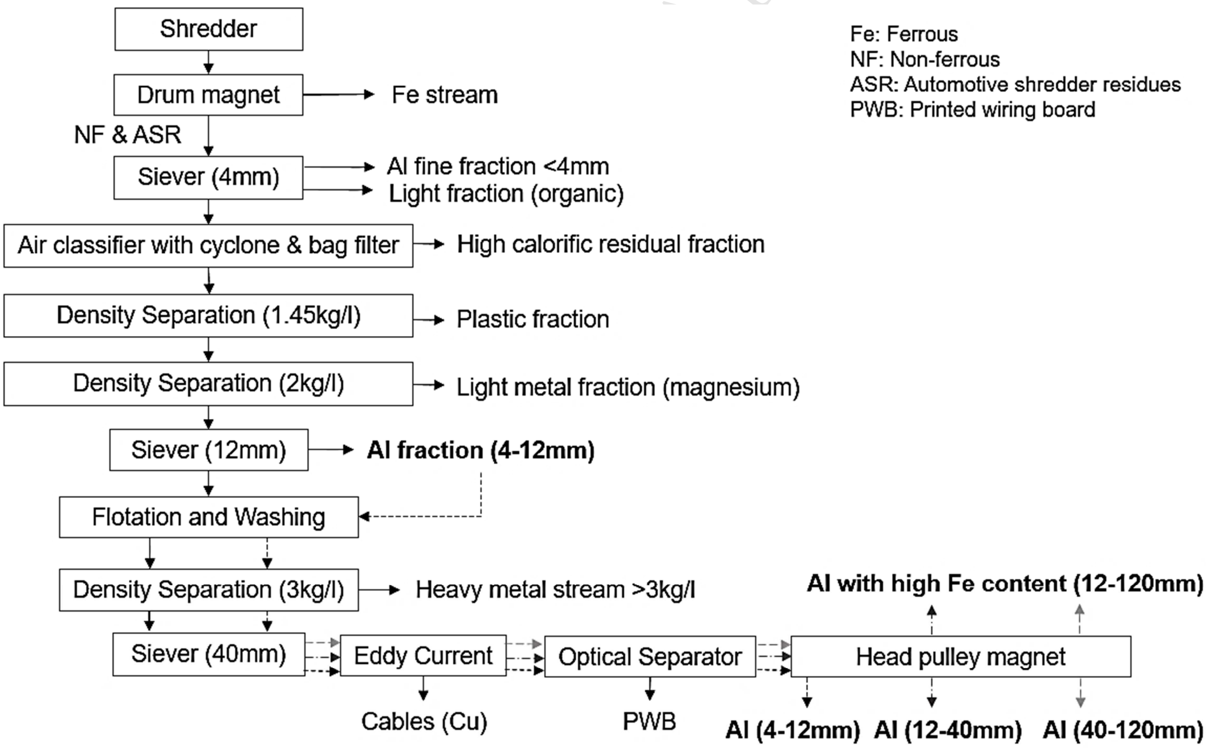

Figure 2: Al material flow in the Belgian recycling facility.

The sorting process targeting Al begins with the density separation after the shredding and magnetic separation. Density separation sorts different materials based on their material densities. It typically starts with separating lighter material fractions (e.g. plastics, foam, rubber, etc.) and is followed by the sorting of materials with higher density. Through density separation at 3kg/l, Al alloys float and can be separated from materials with higher density, such as copper, zinc, and other heavy metals, that sink to the bottom. In some other recycling facilities, Al retrieval through eddy current separation is carried out (Gaustad et al., 2012).

An air classifier is used to remove fine shredder residues targeted for energy recovery before the density separation. This allows the fine mixture of dust, metals, glass, and polymers to be removed before the first density separation for lighter material fraction. Other separation techniques, such as sievers, are also used. The material flow is sorted to different particle sizes based on the siever sizes used at various screening stages. This is a common practice in the recycling industry in Europe to segregate different material grades based on the particle sizes (Cui and Forssberg, 2003).

An eddy current separator, optical separator and head pulley magnet are used to further sort unwanted materials that are still present in the Al flow. The remaining cable wires that did not sink during earlier density separation are further sorted using the eddy current separator. Through this process, an electrical current is induced within the conductive metal flow, and all metals are repelled through the rotor that produces an external magnetic field. Since Al and copper have a different conductivity, and thus produce varying eddy currents, they are ejected to different distances from the rotor. An optical separator is then utilised to further sort the commonly green coloured printed wiring board (PWB) from the grey coloured aluminium. To further remove small particles with ferrous content from the Al flow, a very strong head pulley magnet with a deeper magnetic field is used.

2.2 Sampling Method

The different Al fraction categories recovered from the facility are shown in Table 3. These categories were chosen for sampling to understand the effect of particle sizes on the purity level of various Al fractions, and the extent of impurities due to joints in the different particle sizes. Sampling was also carried out for Al with high Fe content. The collection of a minimum of 10 samples from each Al fraction was performed in accordance with the field sampling guidance for shredded scrap by the

United States Environmental Protection Agency (USEPA, 1993). The field sampling guidance provides information on different sampling methods, estimated sample size, and the statistical analysis methods to accurately approximate the impurity level of different Al fractions. These guidelines were based on previous case studies carried out at different shredder sites.

Table 3: Amount of Al samples taken from each category, and the generated annual amount in the Belgian recycling facility.

Category	**Particle size class (mm)**	**Number of samples**	**Mass range of each sample (kg)**	**Overall sample mass (kg)**	**Annual amount (ton)**
Al with high Fe content	12-120	10	2.685-3.737	32.689	644
Al fraction	40-120	20	2.290-3.896	61.363	6132
Al fraction	12-40	10	1.506-2.408	19.210	4147
Al fraction	4-12	10	1.494-1.947	16.662	1114

There are different field sampling methods for shredded metal scraps on-site based on the guidelines by USEPA. Stockpile sampling, as explained in Figure 3, was chosen in this case study to obtain a more representative sample of the normal shredder output (USEPA, 1993). Al samples were taken from the Al stockpile warehouse where different qualities and particle sizes were stored separately. The bucket used to collect the samples has a diameter of 27.5cm with a height of 22.5cm. Each sample taken only filled up half the bucket. First, Al samples were collected at the edge of pile (location 1) at notch 1 and notch 2. The two notches were then dug to equal depth with the help of a front-loader truck. Finally, samples were gathered at locations 2 to 5 for notch 1 and 2. In total, there were 10 buckets of samples collected for each targeted Al output stream. 20 samples were taken only for the Al fraction 40-120mm to ensure a good representation of the stockpile, since it is the largest fraction produced in the facility.

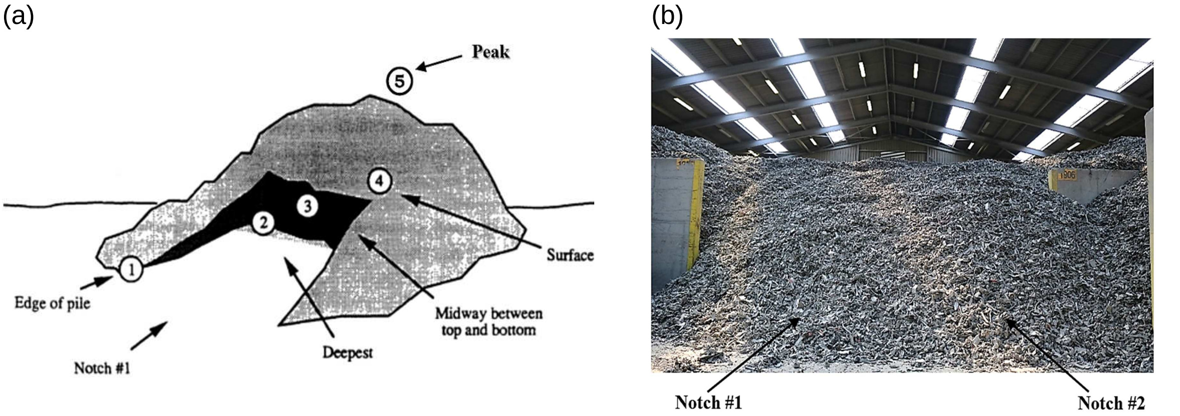

Figure 3: Stockpile sampling of different Al fractions (a) Sampling location for each Al stockpile; (b) Location of notches made for each Al stockpile to carry out sampling.

2.3 Sample Analysis Procedures

The Al with high Fe content fraction was sieved through a 40mm mesh siever to separate particles to two particle size categories: 12-40mm and 40-120mm. This step was carried out to allow comparability with the observations made for the Al fractions of similar particle size classes.

Each particle was weighed and hand-sorted according to the different liberation classifications, as shown in Figure 4 and as follows.

- Liberated Al samples consisting of Al only (Figure 4a).
- Liberated impurities were particles consisting of a single material type other than Al (Figure 4b).
- Unliberated impurities were particles consisting of material combinations other than Al (Figure 4b).
- Unliberated Al samples were particles consisting of Al that was still attached to other material types without the presence of a joint (Figure 4c).
- Unliberated Al samples due to joint were particles consisting of Al that was still attached to other material types with the presence of a joint (Figure 4d).

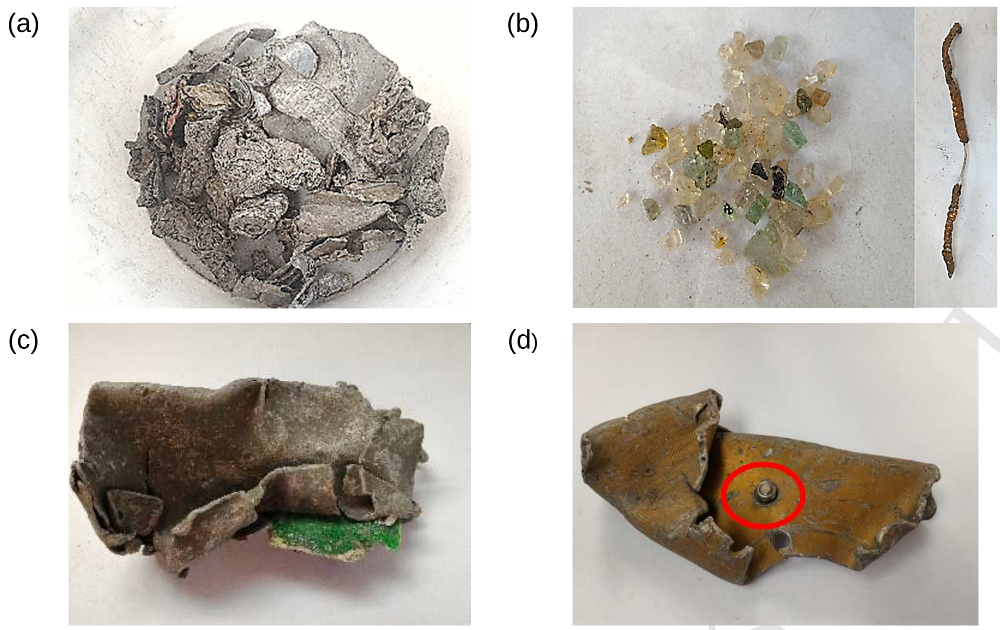

Figure 4: Examples of liberation classification for particles end up in the Al stream. (a) Liberated Al samples (Al particles only); (b) Liberated/unliberated impurities (liberated glass and unliberated Cu-Fe particles); (c) Unliberated Al sample not due to joint (PWB inserted in Al particle); (d) Unliberated Al sample due to joint (screw and bolt attached to Al particle).

Unliberated particles were further separated into their individual materials. The mass of each material was recorded. For cases where further material separation was not possible due to entanglement or rust, the mass of individual materials was calculated using their volumes and average material densities: Al (2745kg/m^3), steel (7825kg/m^3), copper (8595kg/m^3), plastic (1253kg/m^3), rubber (1270kg/m^3), and foam (255kg/m^3) (Callister and Rethwisch, 2013; Gaustad et al., 2012). The types and characteristics of joints causing impurities were observed, and the range of joint sizes, joint material liberation, and the number of rusty joints were recorded quantitatively.

2.4 Environmental Impact Assessment

To evaluate the environmental impacts associated with the quality of different Al scrap fractions collected from the case study, LCA was carried out to assess the dilution and quality losses in remelting the scrap to be reused as Al 6061 alloy (AA6061). During remelting, dilution losses occur due to the need to dilute the residual element concentration (e.g. Fe) with primary Al. To avoid quality losses, alloying elements (e.g. Si and Cu) are added (Paraskevas et al., 2015). The environmental impact assessment only takes into consideration the secondary Al processing of the defined system boundary shown in Figure 5. The wrought AA6061 was chosen as the target secondary alloy since it is widely used in automotive applications and thus, likely to be close to the average composition of the Al scrap retrieved from ELV. To compare the environmental impact of smelting different Al scrap, the functional unit is defined as Al recycling to produce 1 tonne of AA6061. The calculations for the required primary Al for dilution purposes and the additional alloying elements are attached in Appendix A. The credits for subsequent recycling of by-products, such as dross and salt slag, were also taken into consideration.

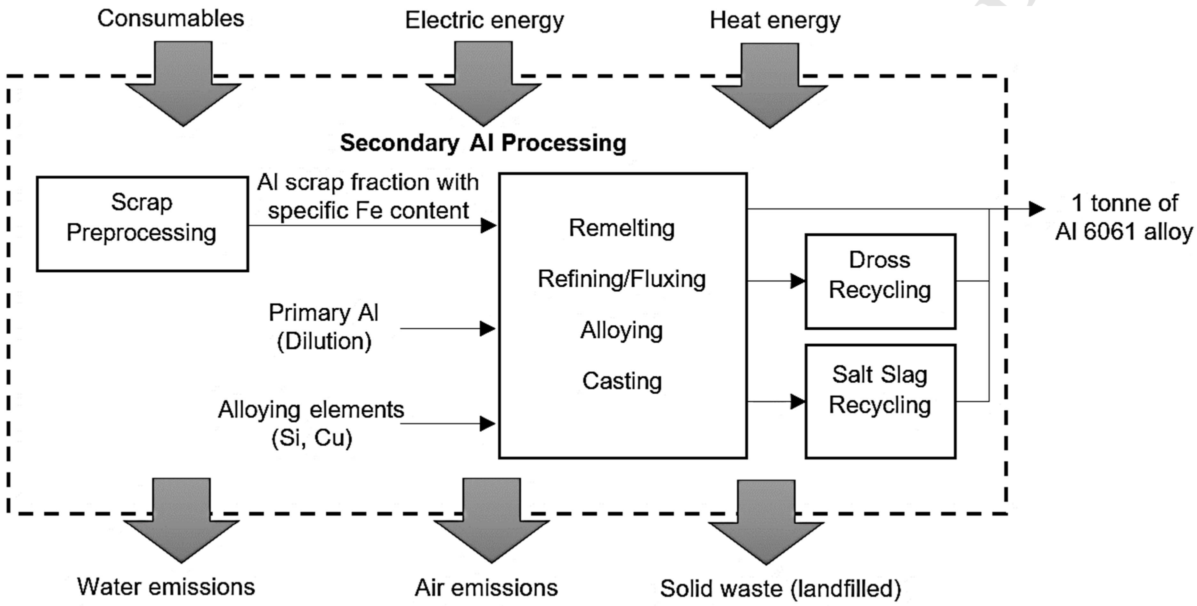

Figure 5: System boundary and functional unit of secondary Al processing for different Al scrap fractions.

GaBi software was used to model all the processes and resources involved during the secondary Al processing. Electricity generation was modelled based on the average electricity consumption mix in Europe. The life cycle inventories were obtained from GaBi Professional database v6.115 and a previous comprehensive report from the Aluminium Association (The Aluminium Association, 2013), as detailed in Table 4. The environmental performance was calculated based on the midpoint categories of the International Reference Life Cycle Data System (ILCD recommendations v1.09). These recommendations were based on the ILCD handbook in accordance with the ISO 14040 series (European Commission et al., 2010; ISO, 2006). Following this method, the midpoint results were normalised to person-equivalent (PE) units—the environmental impact caused by an average European annually. An equal weighting was applied for the midpoint impact categories, and the normalised PE scores for all midpoint categories were added to allow comparison of the overall environmental performance for different Al scrap fractions to achieve 1 tonne of AA6061. The single impact score for climate change (include biogenic carbon) and resource depletion, mineral, fossils and renewables impact are provided in Table 4 due to their significant contribution to the environmental performance.

Table 4: The life cycle inventory data sources for materials and recycling processes, and the respective impact score for climate change (include biogenic carbon) and resource depletion, mineral, fossils and renewables.

Process	**Climate change (PE/ton)**	**Mineral and fossil depletion (PE/ton)**	**Source**	**Description**
Al scrap preprocessing	6.01E-03	3.62E-04	(The Aluminium Association, 2013)	The dataset includes scrap collection, separation, cleaning, and preprocessing.
Al scrap remelting	2.59E-01	1.15E-02	(The Aluminium Association, 2013)	The dataset includes remelting, refining, alloying, and casting of secondary Al. Dross and salt slag recycling are included.
Primary Al ingot	1.08E+00	2.84E-01	GaBi Professional Database v6.115	The dataset includes cradle to gate inventory for primary Al ingot production in Europe.
Primary Cu	4.04E-01	3.56E+02	GaBi Professional Database v6.115	The dataset includes cradle to gate inventory for primary Cu (99.999%) in Germany.
Primary Si	5.45E-01	4.77E-02	GaBi Professional Database v6.115	The dataset includes cradle to gate inventory for primary Si (99%) in global context. The chemical composition is approximated based on Si-2202 (BAIDAO, 2007; SINOGU, 2016).

3 Results

The liberation categories of the collected Al samples from different fractions were studied. The average Al purity of each fraction was determined. The presence of impurities due to joints was further analysed, and the types of joining techniques causing impurities were characterised.

3.1 Al Sample Analysis

The mass distribution of particles in the different liberation categories is shown in Figure 6. Liberated and unliberated impurities were mainly caused by separation errors during the recycling processes, and can be characterised as fine particles (<4mm); materials with similar density range to Al; small and longitudinal heavy metal particles; and materials with density less than Al (<2kg/l). The types of impurities consisted of ferrosilicon fines, glass, PWB, Cu, Fe, wires, plastics, and other light fraction of non-metals. Ferrosilicon fines are an example of fine particles easily trapped in Al samples during the density separation. Glass and PWB have a density range of 2.47-2.54kg/l (Malone and Dolter, 2008) and 1.5-2.89kg/l (Bizzo et al., 2014; Zhang and Forssberg, 1997) respectively that can be similar to Al density. Small heavy metal particles, such as Cu, Fe and wires, with thin and long shapes caused them to be entangled between Al particles during the density separation. Plastics, rubber, fabric, fibrous materials and foam are examples of impurities that were not well separated through density separation at earlier stages. Unliberated Al samples both with or without the presence of joint have higher Al content in the particles by mass and therefore, they were more likely to end up in the Al streams.

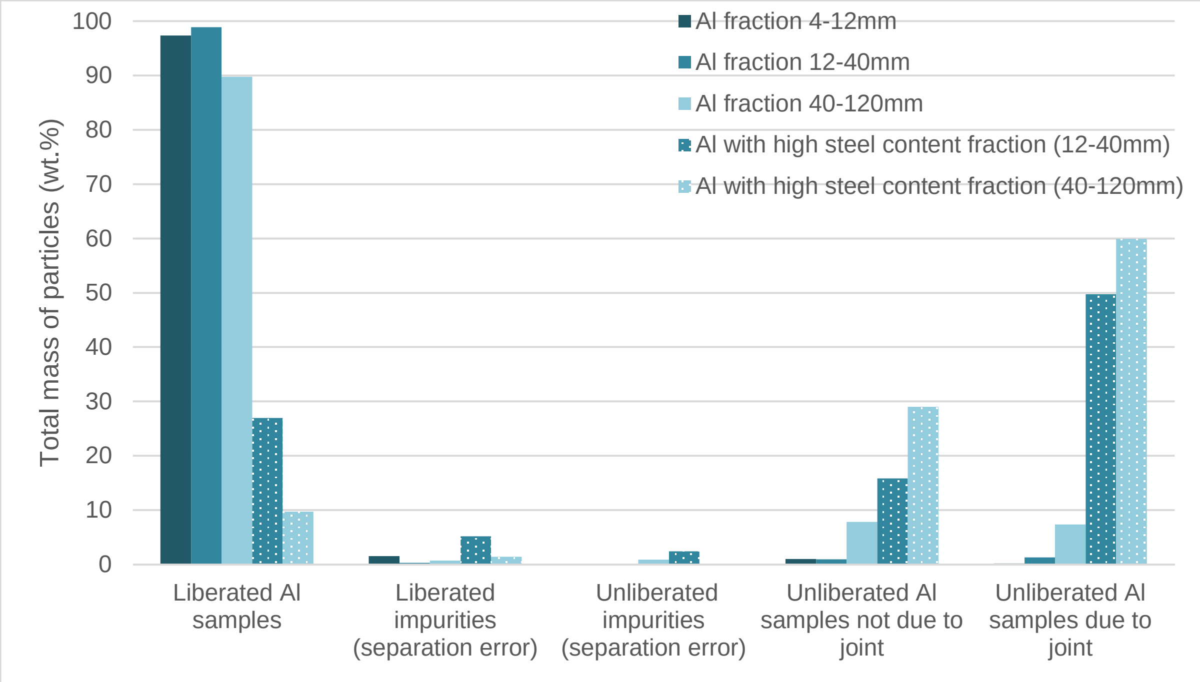

Figure 6: Liberation categories for particles in different Al fractions.

From Figure 6, the total mass of unliberated Al samples both with and without joint is showing an increasing trend when the particle sizes are larger. This observation is valid for both the Al fraction and Al with high steel content fraction. To understand the purity level of Al samples for different particle sizes, the mass fraction of impurities was calculated and the result is shown in Table 5.

Table 5: Al purity for different Al fractions with 95% confidence interval.

Category	**Particle size class (mm)**	**Al purity (wt.%)**
Al with high Fe content fraction	40-120	82.07 ± 3.86
Al with high Fe content fraction	12-40	80.75 ± 3.38
Al fraction	40-120	98.66 ± 0.58
Al fraction	12-40	99.57 ± 0.29
Al fraction	4-12	98.11 ± 0.58

In general, the quality of recycled Al can be separated into two classes: Al purity more than 98%, and Al purity less than 83%. Al purity less than 83% consisted of Al with high steel content fractions that were separated through a strong head pulley magnet as the final separation process in the recycling facility.

Based on the analysis of the shredded samples, smaller particle sizes do not indicate higher Al purity. Al with high Fe content fraction (40-120mm), and Al fraction (12-40mm) have higher Al purity values in their respective categories. The geometry, joint size, and material types of the combined parts also affect the purity levels of Al fractions in different particle sizes. For instance, when a large number of small steel screw fasteners (e.g. steel screw with diameter and length of 2mm and 4mm respectively) are used, the likelihood of Fe impurities due to screw fasteners present in the Al fraction in smaller particle sizes is quite high with respect to mass.

The material types of impurities were identified to understand the extent of contamination in the Al samples. Some of the impurity types can be removed easily during the secondary Al production whereas others, such as Fe, require a dilution process using primary Al. As seen in Table 6, the types of impurities are Fe, Cu, organic and inorganic. It can be observed that the smaller particle size fraction, 4-12mm has a higher impurity level than the 12-40mm fraction due to the material types and the physical characteristics of impurities. These impurities are largely contributed by ferrosilicon fines (consisting of ferrous and silicon), thin and long-shaped wires (consisting of Cu and plastics), small pieces of shattered glass (silicon) and plastics that typically have small dimensions or high brittleness. One of the most undesired tramp elements during Al recycling are Fe impurities (Cho et al., 2015; Paraskevas et al., 2015) due to their detrimental effect on the mechanical properties of Al alloys (Belov et al., 2002). Therefore, this case study focussed on the source of Fe impurities in unliberated samples due to joints to understand the impact of joining choices on the purity level of recycled Al.

Table 6: Types of impurities present in the Al output streams in the Belgian recycling facility.

Category	**Particle size class (mm)**	**Average mass percentage (wt.%)**			
		Fe impurities	**Cu impurities**	**Organic impurities**	**Inorganic impurities**
Al with high Fe fraction	40-120	11.32	0.27	5.82	0.42
Al with high Fe fraction	12-40	9.82	1.38	6.40	1.56
Al fraction	40-120	0.36	0.25	0.71	0.05
Al fraction	12-40	0.03	0.13	0.23	0.06
Al fraction	4-12	0.14	0.26	0.96	0.43

3.2 Observations on the Joint Type Causing Impurities

From the collected Al samples, it was observed that mechanical fastening and adhesive bonding were the two main types of joining techniques causing impurities. The amount of unliberated Al samples due to adhesive bonding was extremely small. They were mostly combinations of Al and lower density materials, such as Al-plastic and Al-foam particles, using lap joint. Lower density materials assisted in breakage during the shredding process due to centrifugal force, and hence, were less likely to cause impurities in the Al samples.

In contrast, mechanical fasteners were the major type of joining method contributing to the presence of Fe impurities in the Al stream, since they are typically made of steel. They were further classified to understand the different types of mechanical fasteners, and how their characteristics contributed to the presence of impurities. Figure 7 shows the various types of mechanical fasteners that were observed in the unliberated Al samples due to joints.

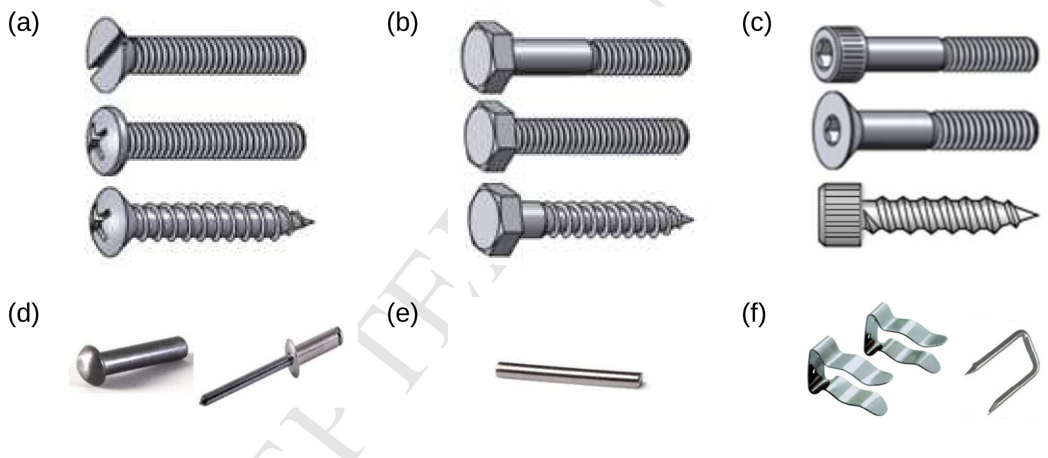

Figure 7: Classification of different mechanical fastening joining methods (Bolt Depot, 2013). (a) Machine screw; (b) Bolt screw; (c) Socket screw; (d) Rivet; (e) Pin; (f) Steel clip.

3.2.1 Al with High Steel Content Fraction (12-120mm)

In Figure 8, it can be observed that the likelihood of Fe impurities due to separation errors decreases for larger particle sizes in Al fraction. The Fe impurities observed in the Al with high Fe content fraction (12-40mm) were mostly small in size due to the inability of the head pulley magnet to pick up small Fe content. There were no Fe impurities due to separation errors observed in the larger particle sizes. Fe impurities that were larger in size have higher likelihood of being separated by the magnetic separator after the shredding process. On the other hand, impurities due to imperfect material liberation were largely caused by structural design, such as enclosures (parts surrounded by different material types) and entanglement (parts that were twisted together or caught in), after the shredding process. Therefore, the likelihood of Fe impurities due to imperfect material liberation increases for larger particle sizes in the Al fraction.

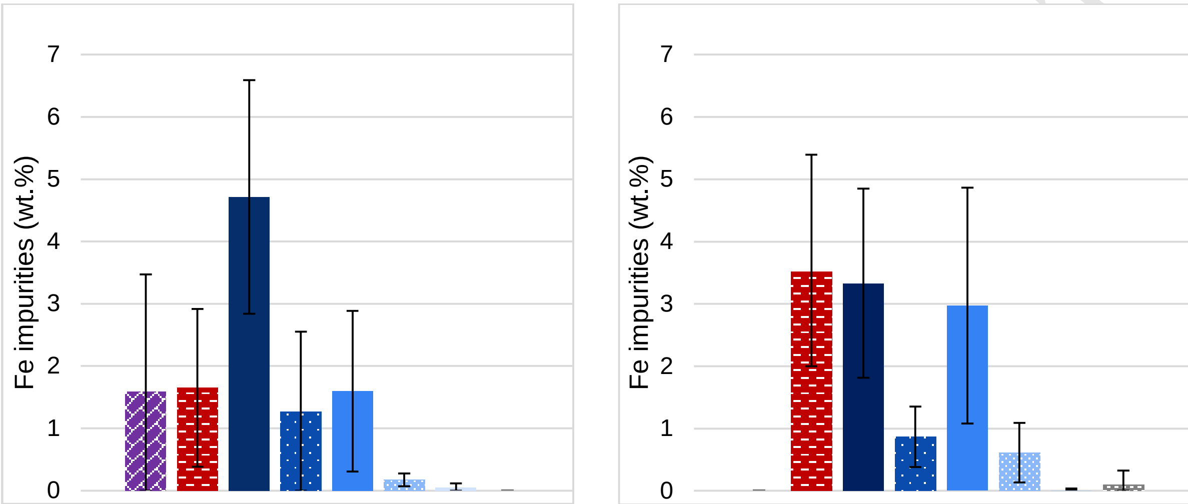

(a) Al with high steel content fraction (12-40mm) without Fe impurities due to unliberated rivets and pins

(b) Al with high steel content fraction (40-120mm) without Fe impurities due to separation errors

Impurities due to separation error
Impurities due to imperfect material liberation
Impurities due to unliberated joint-Machine screw
Impurities due to unliberated joint-Socket screw
Impurities due to unliberated joint-Bolt screw
Impurities due to unliberated joint-Rivet
Impurities due to unliberated joint-Steel clip
Impurities due to unliberated joint-Pin

Figure 8: Fe impurities present in the Al with high steel content fraction with 95% confidence intervals.

There were a variety of mechanical fastener types causing Fe impurities in the Al with high Fe content fractions. Fe impurities observed in smaller particle sizes were caused by unliberated machine screws, socket screws, bolt screws, rivets, and steel clips. No pins were observed for this fraction due to the smoother joining surface that allowed them to be well liberated when shredded to smaller particle sizes. The types of mechanical fasteners causing Fe Impurities in the larger particle sizes were machine screws, socket screws, bolt screws, rivets, steel clips and pin. For both fractions, machine screws were more likely to cause impurities when compared to other mechanical fastener types.

The types of mechanical fasteners causing impurities were further characterised through observation of their physical attributes, as shown in Table 7. The percentages are with respect to the total number of units for each joint type. It is observed that the number of mechanical fasteners in the larger particle sizes were higher compared to the smaller particle sizes except for machine screws and steel clips. Moreover, the fraction with larger particle sizes has a wider range of joint sizes when compared to smaller particle sizes. In spite of that, the number of joint sizes with diameter and length more than 6mm and 10mm respectively (large joint sizes) is similar for both particle size classes. Partial liberation joints, those with more than 50 wt.% of the joint material liberated, were more likely for threaded fasteners such as machine screws and bolt screws. In most cases, the fasteners' head was liberated due to protrusion. Rusty threaded fasteners were also more likely to cause impurities in the Al samples.

Table 7: Characteristics of joint causing Fe impurities in Al with high Fe content fractions.

Joint types	**Total (unit)**	**Joint size (mm)**		**Large joint size (%)**	**Partial liberation (%)**	**Rust (%)**
		Diameter	**Length**			
12-40mm						
Machine screw	101	2-10	3-30	12	9	86
Socket screw	11	4-7	9-36	27	0	64
Bolt screw	16	4-10	8-50	56	0	94
Rivet	13	4-5	3-13	0	0	46
Steel clip	19	2-3	10	0	0	0
40-120mm						
Machine screw	94	2-12	2-30	12	4	76
Socket screw	20	3-9	10-60	30	0	85
Bolt screw	39	3-14	7-125	52	8	76
Rivet	48	5-6	3-50	1	0	48
Steel clip	2	2-3	12	0	0	0
Pin	1		10	0	0	0

3.2.2 Al Fraction (4-120mm)

Similar to Al samples with high Fe content, the likelihood of Fe impurities due to separation errors decreases for larger particles sizes in the Al fraction, as seen in Figure 9, since they can be easily sorted through magnetic separation. In contrast, impurities due to imperfect material liberation could potentially be higher for larger particle sizes, although they were not observed in the Al fraction (12-40mm).

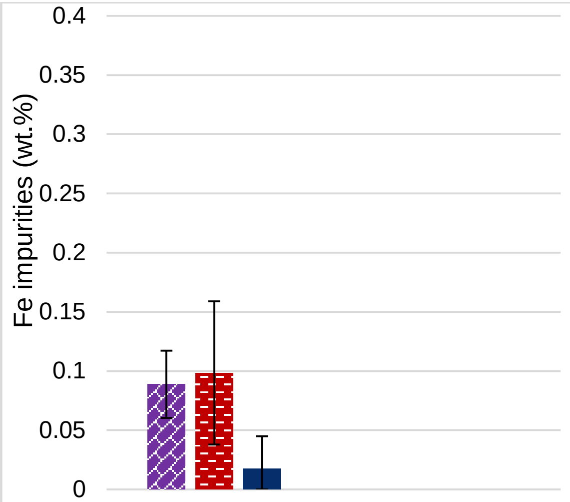

(a) Al fraction (4-12mm) with Fe impurities due to separation errors, imperfect material liberation, and unliberated machine screws

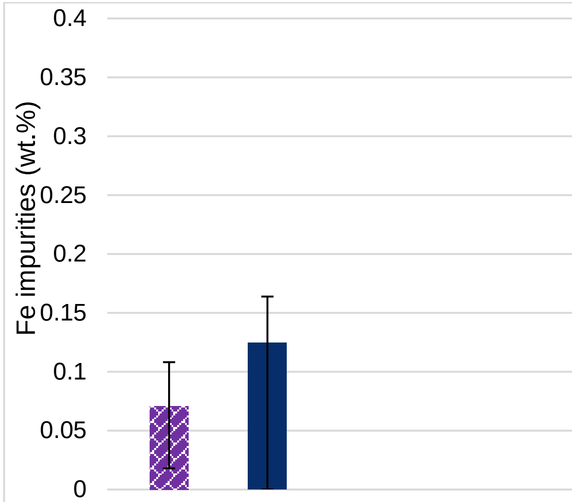

(b) Al fraction (12-40mm) with Fe impurities due to separation errors and unliberated machine screws

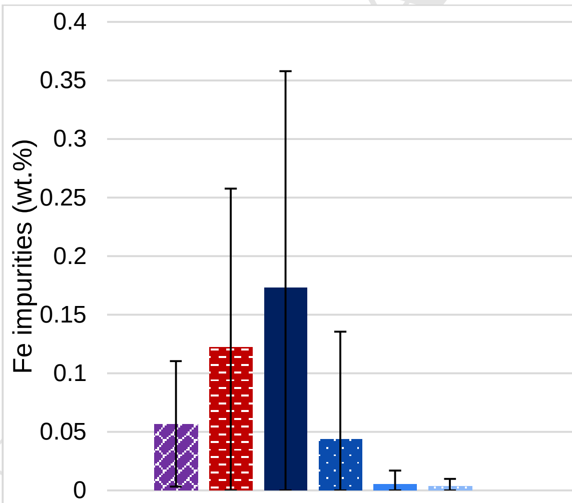

(c) Al fraction (40-120mm) with Fe impurities due to a variety of unliberated joint types

Impurities due to separation error
Impurities due to imperfect material liberation
Impurities due to unliberated joint-Machine screw
Impurities due to unliberated joint-Socket screw
Impurities due to unliberated joint-Bolt screw
Impurities due to unliberated joint-Rivet

Figure 9: Fe impurities present in the Al fraction with 95% confidence intervals.

The likelihood of Fe impurities due to mechanically fastened joints in the Al fraction is higher for larger particle sizes. There was more variety of mechanical fastener types that contribute to the Fe impurities in the Al fraction (40-120mm). Machine screws were the only type of joint causing impurities in the smaller particle sizes, whereas machine screws, socket screws, bolt screws and rivets were observed in Al fraction (40-120mm). Despite the use of a strong head pulley magnet to remove small Fe content, machine screws contaminating the different Al fractions were still present.

Table 8 shows the attributes of mechanical fasteners causing Fe impurities in the different Al fractions. The number of machine screws observed in Al fraction (40-120mm) was larger compared to the fraction containing the smaller particle sizes. However, there was still a small number of machine screws present in this smaller particle size fraction. This was due to the lower magnetic force experienced by small screws located at enclosed spots despite the use of a strong head pulley magnet. In contrast, the presence of mechanical fasteners other than machine screws (socket screws, bolt screws, and rivets) was only seen in Al fraction (40-120mm). Socket screws and bolt screws have a more protruded head compared to machine screws that facilitate liberation during the shredding process. On the other hand, rivets have a smooth surface that allows them to be easily set free when shredded into smaller particle sizes. The likelihood of impurities due to larger joint sizes or of partial liberation is higher for larger particle sizes particularly for the machine screw fastener type.

Table 8: Characteristics of joint causing Fe impurities in Al fractions.

Joint types	**Total (unit)**	**Joint size (mm)**		**Large joint size (%)**	**Partial liberation (%)**	**Rust (%)**
		Diameter	**Length**			
4-12mm						
Machine screw	2	3-4	8	0	0	100
12-40mm						
Machine screw	1	5	20	0	0	100
40-120mm						
Machine screw	17	3-8	5-25	18	12	50
Socket screw	1	4	18	0	0	0
Bolt screw	2	4	11-12	0	0	50
Rivet	2	5	7	0	0	0

4 Environmental Impact Assessment Results

From the LCA results presented in Figure 10, the total environmental impact for Al with high Fe scrap fractions (both particle sizes) has increased by at least 28 times in comparison to the Al scrap fractions (4-12mm, 12-40mm, and 40-120mm). This is caused by the higher concentration of Fe, that can be considered as impurities rather than useful alloying elements, and the addition of Si and Cu alloying elements to produce AA6061. The contribution of different midpoint impact categories for the different Al scrap fractions to produce 1 tonne of AA6061 is provided in Appendix A. The use of primary Al as dilution agent is the major contributor to the environmental impact for Al scrap with high Fe content with an impact share of at least 92%, as supported in other studies (Amini et al., 2007; Paraskevas et al., 2015). To achieve higher purity wrought Al alloy, a substantial amount of primary Al is required for the dilution of these streams, and alloying elements are added to meet the compositional limits. This results in scrap underutilisation since only 3-6wt.% of the produced AA6061 consists of recycled Al scrap. The use of primary Al for dilution can be minimised by using other high purity scrap streams and optimised Al scrap blending (Paraskevas et al., 2015).

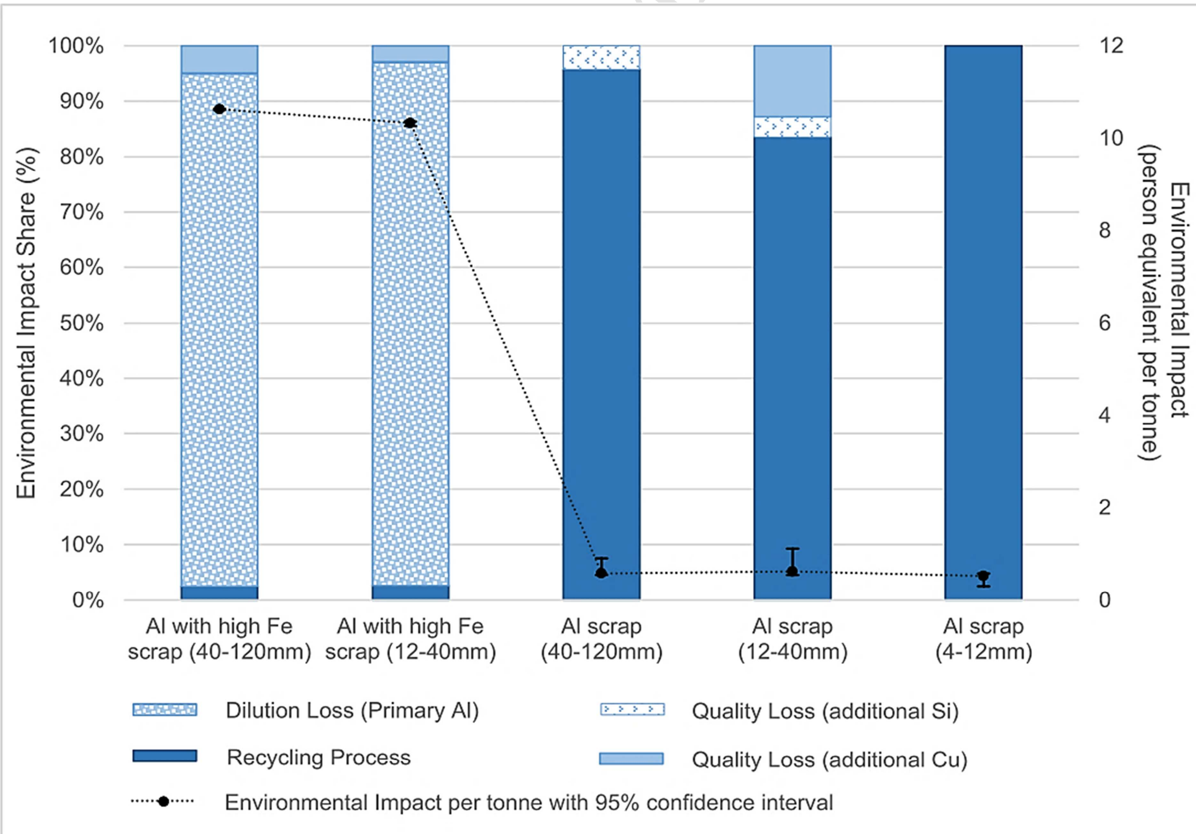

Figure 10: Total environmental impact and the share of recycling, dilution and quality losses for different Al scrap fractions to achieve 1 tonne of AA6061.

A sensitivity analysis was carried out to assess the influence of varying element values for different Al scrap fractions. The range of values for Fe, Si and Cu elements are shown in Table 9. As can be seen from Figure 10, the total environmental impact is sensitive to the range of values for Fe, Si and Cu in different Al scrap fractions. It is shown that the margin of error for the total environmental impact can be up to ±0.5 person equivalent per tonne. However, the trend of the total environmental impact for the range of element values is largely unaffected. The total environmental impact for Al with high Fe scrap fractions is greatly influenced by the dilution losses. In contrast, the total environmental impact for Al scrap fractions is largely contributed by recycling process and quality losses since no dilution losses occur. Despite the sensitivity to the range of Fe, Si and Cu values, the negative impact of the Al scrap fractions is insignificant compared to Al scrap with high Fe content.

Table 9: The range of values for Fe, Si and Cu present in the different Al scrap fractions with 95% confidence interval.

Category	**Particle sizes (mm)**	**Fe (wt.%)**		**Si (wt.%)**		**Cu (wt.%)**	
		min	**max**	**min**	**max**	**min**	**max**
Al with high Fe fraction	40-120	9.95	12.69	0.00	0.94	0.00	0.46
Al with high Fe fraction	12-40	7.12	12.53	0.00	3.51	0.51	2.24
Al fraction	40-120	0.03	0.68	0.00	0.11	0.06	0.46
Al fraction	12-40	0.00	0.06	0.03	0.09	0.00	0.28
Al fraction	4-12	0.07	0.20	0.27	0.54	0.14	0.38

As can be seen from Figure 11, about 70% of the total impact share of dilution losses for Al scrap with high Fe content is caused by unliberated joints. Dilution losses due to material separation errors can only be observed for Al with high Fe scrap in smaller particle sizes due to the presence of silicon from the shattered glass. The environmental evaluation based on the case study data shows that the dilution and quality loss impacts are tightly-linked to the quality or purity level of the recovered Al streams resulting from material liberation. The high Fe content due to improper material liberation has become a limiting factor for the recyclability of the Al streams. It is worth noting that the environmental performance may vary according to the efficiency of recycling technologies used in different countries.

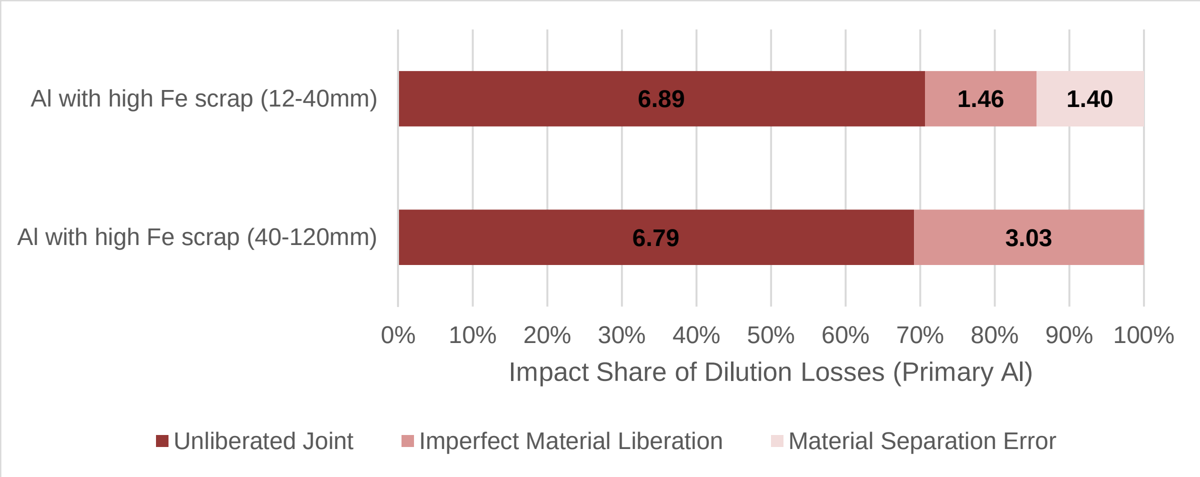

Figure 11: The impact share of dilution losses (primary Al addition) and the environmental impact (person equivalent per tonne) due to liberation categories.

5 Discussion

The annual Al output streams in the Belgian recycling facility are shown in Table 10. The material composition in each Al stream is estimated from the performed sampling, and subjected to the variation based on the 95% confidence interval. Despite the large variance for certain tramp elements in different Al output streams, the impact on the environmental performance is insignificant. Al fractions (12-40mm) and (40-120mm) are the two largest fractions with high Al purity levels of 99.57% and 98.66% respectively, whereas the Al with high Fe content fraction has the lowest annual amount with low Al purity level of 81.28% (combination of both particle sizes). With the increasing complexity of multi-material designs, particularly in the automotive sector which is one of the largest consumers of Al, it is projected that the Al with high Fe content fraction will be growing and thus, lead to the reduction of the Al fraction with higher purity (Soo et al., 2015, 2016).

Table 10: Estimated material composition for the Belgian recycling facility's annual Al output streams based on the extrapolation of sampling results.

Material type	**Al with high Fe content fraction (12-120mm)**		**Al fraction (40-120mm)**		**Al fraction (12-40mm)**		**Al fraction (4-12mm)**	
	ton	***wt. %***	***ton***	***wt. %***	***ton***	***wt. %***	***ton***	***wt. %***
Al	523.46	81.28	6048.50	98.64	4128.60	99.56	1093.00	98.11
PWB	2.09	0.32	3.14	0.05	1.45	0.03	6.04	0.54
Wire	4.21	0.65	18.80	0.31	2.41	0.06	2.72	0.24
Cu	0.62	0.10	7.60	0.12	4.24	0.10	0.61	0.06
Plastic/composite	12.13	1.88	19.44	0.32	3.87	0.09	3.57	0.32
Rubber	18.26	2.84	6.71	0.11	2.67	0.06	0.20	0.02
Steel	75.82	11.77	21.39	0.35	0.73	0.02	1.29	0.12
Foam	0.57	0.09	0.46	0.01	0.21	0.01	0	0
Fabric	2.19	0.34	2.16	0.04	0	0	0	0
Synthetic leather	0.28	0.04	0	0	0	0	0	0
Glass	0	0	0	0	0	0	5.06	0.45
Fibrous material	2.66	0.41	0	0.41	0	0	0.40	0.04
Ferrosilicon fine	1.70	0.26	3.86	0.06	2.80	0.07	1.16	0.10
TOTAL:	**644**	**100**	**6132**	**100**	**4147**	**100**	**1114**	**100**

5.1 Observational Study Outcomes

From the analysed samples, most of the Fe impurities were due to unliberated joints particularly for Al with high Fe fractions, and Al particles of larger sizes, as seen in Table 11. Particles with unliberated joints in the Al with high Fe fractions have contributed at least by 69% to the total Fe impurities. When the particle sizes for different Al fractions decrease, the total Fe impurities due to unliberated joints decrease by at least 33%. Therefore, smaller particle sizes can assist in reducing Fe impurities due to unliberated joints. However, the proportion of Fe impurities due to separation errors or imperfect material liberation is higher for Al fractions with smaller particle sizes. The presence of these impurities is strongly influenced by the material structural design, joint size used, and the efficiency of the recycling processes in sorting small to fine particles. Thus, additional loops in Fe impurity removal or adjustment of the installation with strong magnets could assist in reducing material separation errors for smaller particle sizes.

Table 11: The proportion of Fe impurities due to separation error, imperfect material liberation and unliberated joint.

Category	Particle size class (mm)	Total Fe impurities (wt.%)		
		Separation error	Imperfect material liberation	Unliberated joint
Al with high Fe fraction	40-120	0	3.52	7.88
Al with high Fe fraction	12-40	1.41	1.47	6.94
Al fraction	40-120	0.04	0.08	0.24
Al fraction	12-40	0.03	0	0.01
Al fraction	4-12	0.06	0.07	0.01

5.2 Recommendations to Improve Al Scrap Quality

Based on the case study observations, the suggestions to improve the quality of Al recycling from ecodesign (materials and connections) and recycling process perspectives are as follows.

Ecodesign

- Encourage the use of low cost disassembly embedded design, such as the use of active fasteners (connections that can be unfastened simultaneously through a specific trigger or a combination of triggers), to maximise the material/part reuse without compromising the product use phase (Duflou et al., 2008; Peeters et al., 2015; Peeters et al., 2017).
- Encourage the use of mechanical fasteners with greater protrusion and smoother joining surface, such as socket screws, rivets and pins, to ease particle liberation.
- Avoid the use of machine screws. Otherwise, minimise the total number and sizes of joints particularly for machine screws to reduce the mass of Fe impurities.

Recycling processes

- Encourage shredding of particles into smaller sizes to decrease the presence of impurities due to mechanical fastening joints and imperfect liberation.
- Encourage the use of strong head pulley magnets to further sort small Fe content particularly for Al particles that still contain smaller size mechanical fastening joints. This process is not commonly used in recycling facilities.

- Encourage the use of more efficient sorting processes for PWB, Cu and wires to refine Al scrap after density separation, such as wet shaker tables (Jordão et al., 2016), kinetic gravity separators (Rem, 2009), and nail roll separators (Fabrizi et al., 2003).

The feasibility of the proposed recommendations can be influenced by other factors, such as the economic aspects and legislative boundaries (Soo et al., 2017). Recycling of high purity materials can be affected by the additional recycling costs, the profit of the end products, or the generated mass or volume of different quality scrap fractions. In addition, a governmental role can also be of importance through the imposing of a minimum purity level required for outputs from recycling activities.

6 Conclusions and Future Work

Despite the rigorous recycling processes used in the Belgian recycling facility, unliberated joints are one of the major contributors to the presence of Fe impurities in the Al output streams, particularly for Al with high steel content fractions. The Fe content level highly influences the recyclability of Al scrap; thus, the environmental impact of dilution and quality losses during Al recycling needs to be integrated into LCA for better-informed decisions towards closed-loop recycling.

The main type of joining techniques causing impurities in the Al streams are mechanical fasteners, such as machine screws, socket screws, bolt screws and rivets, which are commonly used for assembling Al with other materials. Although adhesive bonding was also observed to cause impurities in the Al particles, these were relatively small and almost negligible when compared to the effects of mechanical fastening joints.

Based on the observations of the collected samples, machine screws were the major type of mechanical fasteners causing Fe impurities in different Al fractions due to their joint characteristics. This was consistently observed for various particle sizes. Machine screws are normally less protruded compared to other mechanical fasteners, such as bolt screw, and socket screw. A higher level of protrusion eases liberation during the shredding process. In addition, machine screws that were smaller in size, and corroded due to moisture will make particle liberation more challenging. There were also cases of partial liberation due to the threaded structure that further hindered full material liberation.

Unliberated Al samples due to the presence of joints are less likely for smaller shredder output fractions with respect to the total mass of particles. It was found that smaller particle sizes ease liberation of Fe impurities from the joints. However, when considering the Al purity level for different particle sizes, they do not indicate a higher purity level for smaller particle sizes. This was largely caused by the increasing proportion of Fe impurities due to separation errors and imperfect material liberation. Although sorting of Al scrap into different fractions is proven to be effective in obtaining high quality Al in most European countries, it is important to understand the quality of recycled Al scrap in high consumption countries, such as in China (RBC Capital Markets, 2015), from a global perspective.

It can be concluded that the choice of joining techniques during the design phase has a significant impact on the environmental performance during the EoL phase. The share of unliberated joints causing the environmental impact due to dilution losses in the Al scrap with high Fe content is the highest compared to material separation errors and imperfect material liberation. Dilution losses cause a significant environmental impact and reduce the avoided environmental impact during Al recycling.

Acknowledgement

The authors would like to thank the Belgian recycling facility for their participation in this case study. This study is supported by the Commonwealth Government CRC Program (AutoCRC), the Australian National University, and the Centre for Industrial Management, University of Leuven.

Appendix A. Supplementary Data

The supplementary data related to this article is as attached.

References

Amini, S.H., Remmerswaal, J.A.M., Castro, M.B., Reuter, M.A., 2007. Quantifying the quality loss and resource efficiency of recycling by means of exergy analysis. J. Clean. Prod. 15, 907–913. doi:10.1016/j.jclepro.2006.01.010

BAIDAO, 2007. Silicon metal 2202 [WWW Document]. URL http://siliconmetal.net/siliconmetal2202.htm (accessed 6.8.17).

Barnes, T.A., Pashby, I.R., 2000a. Joining techniques for aluminium spaceframes used in automobiles: Part I—solid and liquid phase welding. J. Mater. Process. Technol. 99, 62–71. doi:10.1016/S0924-0136(99)00367-2

Barnes, T.A., Pashby, I.R., 2000b. Joining techniques for aluminium spaceframes used in automobiles: Part II—adhesive bonding and mechanical fasteners. J. Mater. Process. Technol. 99, 72–79. doi:10.1016/S0924-0136(99)00361-1

Belov, N.A., Aksenov, A.A., Eskin, D.G., 2002. Iron in aluminium alloys: impurity and alloying element. CRC Press.

Bizzo, W.A., Figueiredo, R.A., de Andrade, V.F., 2014. Characterization of printed circuit boards for metal and energy recovery after milling and mechanical separation. Materials 7, 4555–4566. doi:10.3390/ma7064555

Bolt Depot, 2013. Bolt Depot - Printable Fastener Tools [WWW Document]. URL https://www.boltdepot.com/fastener-information/Printable-Tools/Default.aspx (accessed 2.13.17).

Bras, B., 2005. Recycling Guidelines-Course notes for ME4171 - Environmentally Conscious Design and Manufacture. Atlanta, Georgia.

Callister, W.D., Rethwisch, D.G., 2013. Materials Science and Engineering: An Introduction, 9th Edition: Ninth Edition.

Carle, D., Blount, G., 1999. The suitability of aluminium as an alternative material for car bodies. Mater. Des. 20, 267–272. doi:10.1016/S0261-3069(99)00003-5

Castro, M.B., Remmerswaal, J.A.M., Brezet, J.C., Van Schaik, A., Reuter, M.A., 2005. A simulation model of the comminution–liberation of recycling streams: Relationships between product design and the liberation of materials during recycling. Int. J. Miner. Process. 75, 255–281. doi:10.1016/j.minpro.2004.09.001

Castro, M.B.G., Remmerswaal, J.A.M., Reuter, M.A., Boin, U.J.M., 2004. A thermodynamic approach to the compatibility of materials combinations for recycling. Resour. Conserv. Recycl. 43, 1–19. doi:10.1016/j.resconrec.2004.04.011

Cho, T.T., Meng, Y., Sugiyama, S., Yanagimoto, J., 2015. Separation technology of tramp elements in aluminium alloy scrap by semisolid processing. Int. J. Precis. Eng. Manuf. 16, 177–183. doi:10.1007/s12541-015-0023-3

Cui, J., Forssberg, E., 2003. Mechanical recycling of waste electric and electronic equipment: a review. J. Hazard. Mater. 99, 243–263. doi:10.1016/S0304-3894(03)00061-X

Cui, X., Zhang, H., Wang, S., Zhang, L., Ko, J., 2011. Design of lightweight multi-material automotive bodies using new material performance indices of thin-walled beams for the material selection with crashworthiness consideration. Mater. Des. 32, 815–821. doi:10.1016/j.matdes.2010.07.018

Cullen, J.M., Allwood, J.M., 2013. Mapping the global flow of aluminum: From liquid aluminum to end-use goods. Environ. Sci. Technol. 47, 3057–3064. doi:10.1021/es304256s

Davies, G., 2012. Materials for automobile bodies. Butterworth-Heinemann.

Duflou, J.R., Seliger, G., Kara, S., Umeda, Y., Ometto, A., Willems, B., 2008. Efficiency and feasibility of product disassembly: A case-based study. CIRP Ann. - Manuf. Technol. 57, 583–600. doi:10.1016/j.cirp.2008.09.009

European Aluminium Association, 2013. The Aluminium Automotive Manual. European Aluminium Association.

European Commission, Joint Research Centre, Institute for Environment and Sustainability, 2010. ILCD Handbook - General guide for Life Cycle Assessment-Detailed guidance. Publications Office of the European Union, Luxembourg.

Fabrizi, L., De Jong, T.P.R., Bevilacqua, P., 2003. Wire separation from automotive shredder residue. Phys. Sep. Sci. Eng. 12, 145–165. doi:10.1080/14786470310001608428

Ferrão, P., Amaral, J., 2006. Design for recycling in the automobile industry: new approaches and new tools. J. Eng. Des. 17, 447–462. doi:10.1080/09544820600648039

Froelich, D., Haoues, N., Leroy, Y., Renard, H., 2007. Development of a new methodology to integrate ELV treatment limits into requirements for metal automotive part design. Miner. Eng., Selected papers from Material, Minerals & Metal Ecology ’06, Cape Town, South Africa, November 2006 20, 891–901. doi:10.1016/j.mineng.2007.04.019

Gaustad, G., Olivetti, E., Kirchain, R., 2012. Improving aluminum recycling: A survey of sorting and impurity removal technologies. Resour. Conserv. Recycl. 58, 79–87. doi:10.1016/j.resconrec.2011.10.010

Goede, M., Stehlin, M., Rafflenbeul, L., Kopp, G., Beeh, E., 2008. Super Light Car—lightweight construction thanks to a multi-material design and function integration. Eur. Transp. Res. Rev. 1, 5–10. doi:10.1007/s12544-008-0001-2

Groche, P., Wohletz, S., Brenneis, M., Pabst, C., Resch, F., 2014. Joining by forming—a review on joint mechanisms, applications and future trends. J. Mater. Process. Technol. 214, 1972–1994. doi:10.1016/j.jmatprotec.2013.12.022

Grote, K.H., Antonsson, E.K. (Eds.), 2009. Springer handbook of mechanical engineering. Springer Science & Business Media.

Güngör, A., 2006. Evaluation of connection types in design for disassembly (DFD) using analytic network process. Comput. Ind. Eng. 50, 35–54. doi:10.1016/j.cie.2005.12.002

Hatayama, H., Daigo, I., Matsuno, Y., Adachi, Y., 2012. Evolution of aluminum recycling initiated by the introduction of next-generation vehicles and scrap sorting technology. Resour. Conserv. Recycl. 66, 8–14. doi:10.1016/j.resconrec.2012.06.006

Hirsch, J., 2011. Aluminium in innovative light-weight car design. Mater. Trans. 52, 818–824. doi:10.2320/matertrans.L-MZ201132

International Aluminium Institute, 2017. Global Aluminium Flow Model - 2015.

ISO, 2006. ISO 14040: environmental management—life cycle assessment—principles of framework. International Organisation for Standardisation (ISO).

Jordão, H., Sousa, A.J., Carvalho, M.T., 2016. Optimization of wet shaking table process using response surface methodology applied to the separation of copper and aluminum from the fine fraction of shredder ELVs. Waste Manag. 48, 366–373. doi:10.1016/j.wasman.2015.10.006

Kriwet, A., Zussman, E., Seliger, G., 1995. Systematic integration of design-for-recycling into product design. Int. J. Prod. Econ., Collaborative integration 38, 15–22. doi:10.1016/0925-5273(95)99062-A

Liu, G., Müller, D.B., 2012. Addressing sustainability in the aluminum industry: a critical review of life cycle assessments. J. Clean. Prod. 35, 108–117. doi:10.1016/j.jclepro.2012.05.030

Luttropp, C., Lagerstedt, J., 2006. EcoDesign and The Ten Golden Rules: generic advice for merging environmental aspects into product development. J. Clean. Prod. 14, 1396–1408. doi:10.1016/j.jclepro.2005.11.022

Malone, L.J., Dolter, T., 2008. Basic concepts of chemistry. John Wiley & Sons.

Martchek, K., 2006. Modelling more sustainable aluminium. Int. J. Life Cycle Assess. 11, 34–37. doi:10.1065/lca2006.01.231

Meschut, G., Janzen, V., Olfermann, T., 2014. Innovative and highly productive joining technologies for multi-material lightweight car body structures. J. Mater. Eng. Perform. 23, 1515–1523. doi:10.1007/s11665-014-0962-3

Miller, W.S., Zhuang, L., Bottema, J., Wittebrood, A.., De Smet, P., Haszler, A., Vieregge, A., 2000. Recent development in aluminium alloys for the automotive industry. Mater. Sci. Eng. A 280, 37–49. doi:10.1016/S0921-5093(99)00653-X

Mirdamadi, M., Korchnak, G., 2006. Great automotive designs enabled by advances in adhesive bonding. Great Design in Steel.

Mori, K.I., Bay, N., Fratini, L., Micari, F., Tekkaya, A.E., 2013. Joining by plastic deformation. CIRP Ann. - Manuf. Technol. 62, 673–694. doi:10.1016/j.cirp.2013.05.004

Muchová, L., Eder, P., 2010. End-of-waste criteria for aluminium and aluminium alloy scrap: technical proposals. Inst. Prospect. Technol. Stud. Publ. Off. Eur. Union Luxemb. 66.

Nakajima, K., Takeda, O., Miki, T., Matsubae, K., Nakamura, S., Nagasaka, T., 2010. Thermodynamic analysis of contamination by alloying elements in aluminum recycling. Environ. Sci. Technol. 44, 5594–5600. doi:10.1021/es9038769

Nappi, C., 2013. The global aluminium industry 40 years from 1972. World Alum. 1–27.

Norgate, T.E., Jahanshahi, S., Rankin, W.J., 2007. Assessing the environmental impact of metal production processes. J. Clean. Prod., From Cleaner Production to Sustainable Production and Consumption in Australia and New Zealand: Achievements, Challenges, and Opportunities 15, 838–848. doi:10.1016/j.jclepro.2006.06.018

Paraskevas, D., Kellens, K., Dewulf, W., Duflou, J.R., 2015. Environmental modelling of aluminium recycling: a Life Cycle Assessment tool for sustainable metal management. J. Clean. Prod., Decision-support models and tools for helping to make real progress to more sustainable societies 105, 357–370. doi:10.1016/j.jclepro.2014.09.102

Peeters, J.R., Vanegas, P., Dewulf, W., Duflou, J.R., 2017. Economic and environmental evaluation of design for active disassembly. J. Clean. Prod. 140, Part 3, 1182–1193. doi:10.1016/j.jclepro.2016.10.043

Peeters, J.R., Vanegas, P., Van den Bossche, W., Devoldere, T., Dewulf, W., Duflou, J.R., 2015. Elastomer-based fastener development to facilitate rapid disassembly for consumer products. J. Clean. Prod. 94, 177–186. doi:10.1016/j.jclepro.2015.01.081

RBC Capital Markets, 2015. Metal Prospects: Aluminium Market Outlook - Fourth Quarter 2015.

RDC Environment, 2015. Confidentiële data Galloo 2014.

Reck, B.K., Graedel, T.E., 2012. Challenges in Metal Recycling. Science 337, 690–695. doi:10.1126/science.1217501

Rem, P., 2009. WRAP MDD018/23 WEEE separation techniques - Kinetic Gravity Separator trial report. Delft University of Technology.

Reuter, M.A., 2011. Limits of Design for Recycling and “Sustainability”: A Review. Waste Biomass Valorization 2, 183–208. doi:10.1007/s12649-010-9061-3

SINOGU, 2016. Silicon Metal 2202 3303 553 441 [WWW Document]. URL http://www.sinogu.com/archives/high-quality-silicon-metal-2202-3303-553-441.html (accessed 6.8.17).

Soo, V.K., Compston, P., Doolan, M., 2016. Is the Australian Automotive Recycling Industry Heading towards a Global Circular Economy?–A Case Study on Vehicle Doors. Procedia CIRP 48, 10–15. doi:10.1016/j.procir.2016.03.099

Soo, V.K., Compston, P., Doolan, M., 2015. Interaction between new car design and recycling impact on life cycle assessment. Procedia CIRP 29, 426–431. doi:10.1016/j.procir.2015.02.055

Soo, V.K., Peeters, J., Compston, P., Doolan, M., Duflou, J.R., 2017. Comparative Study of End-of-Life Vehicle Recycling in Australia and Belgium. Procedia CIRP 61, 269–274. doi:10.1016/j.procir.2016.11.222

The Aluminium Association, 2013. The Environmental Footprint of Semi-finished Aluminium Products in North America, A life cycle assessment report.

U.S. Department of Energy, 2013. Use of Lightweight Materials is on the Rise [WWW Document]. Veh. Technol. Off. URL https://www1.eere.energy.gov/vehiclesandfuels/facts/2013_fotw786.html (accessed 2.24.14).

USEPA, 1993. Sampling guidance for scrap metal shredders-field manual.

Van Schaik, A., Reuter, M.A., 2007. The use of fuzzy rule models to link automotive design to recycling rate calculation. Miner. Eng., Selected papers from Material, Minerals & Metal Ecology ’06, Cape Town, South Africa, November 2006 20, 875–890. doi:10.1016/j.mineng.2007.03.016

VDI 2243, 1993. Konstruieren Recyclinggerechter Technischer Produkte (Designing Technical Products for ease of Recycling). Germany.

Volkswagen Group, 2009. Innovative Developments for Lightweight Vehicle Structures. Wolfsburg, Germany.

Worrell, E., Reuter, M.A. (Eds.), 2014. Handbook of Recycling: State-of-the-art for Practitioners, Analysts, and Scientists. Newnes.

Zhang, S., Forssberg, E., 1997. Mechanical separation-oriented characterization of electronic scrap. Resour. Conserv. Recycl. 21, 247–269. doi:10.1016/S0921-3449(97)00039-6

Highlights

- Identified the types of joining techniques causing impurities in the Al streams.
- Characterised the joints causing Fe impurities in the Al streams.
- Recycling efficiency of Al was measured through an industrial trial in Europe.
- Identified the linkage between particle sizes and impurities due to joints.
- Assessed the environmental impact of dilution and quality losses due to joints.